

1 **Deposit-feeding of *Nonionellina labradorica* (foraminifera) from an**
2 **Arctic methane seep site and possible association with a**
3 **methanotroph**

4 Christiane Schmidt^{1,2,3}, Emmanuelle Geslin¹, Joan M Bernhard⁴, Charlotte LeKieffre^{1,5}, Mette
5 Marianne Svenning^{2,6}, Helene Roberge^{1,7}, Magali Schweizer¹, Giuliana Panieri²

6 ¹LPG, Laboratoire de Planétologie et Géosciences, Univ of Angers, Nantes Université, Le Mans Univ CNRS, LPG,
7 SFR QUASAV, Angers, 49000, France

8 ²CAGE, Centre for Arctic Gas Hydrate, Environment and Climate, UiT, The Arctic University of Norway, Tromsø,
9 9010, Norway

10 ³ZMT, Leibniz Centre for Tropical Marine Research, Bremen, 28359, Germany

11 ⁴Woods Hole Oceanographic Institution, Geology & Geophysics Department, Woods Hole, 02543, MA, USA

12 ⁵Cell and Plant Physiology Laboratory, CNRS, CEA, INRAE, IRIG, Université Grenoble Alpes, Grenoble, 38054
13 France

14 ⁶Department of Arctic and Marine Biology, UiT, The Arctic University of Norway, Tromsø, 9037, Norway

15 ⁷Université de Nantes, CNRS, Institut des Matériaux Jean Rouxel, IMN, Nantes, 44000 France

16

17 *Correspondence to* Christiane Schmidt christiane.schmidt@leibniz-zmt.de

18

19

20 **Abstract.** Several foraminifera are deposit feeders that consume organic detritus (dead particulate
21 organic material with entrained bacteria). However, the role of such foraminifera in the benthic
22 food-web remains understudied. Foraminifera feeding on methanotrophic bacteria, which are ^{13}C -
23 depleted, may cause negative cytoplasmic and/or calcitic $\delta^{13}\text{C}$ values. To test whether the
24 foraminiferal diet includes methanotrophs, we performed a short-term (20-h) feeding experiment
25 with *Nonionellina labradorica* from an active Arctic methane-emission site (Storfjordrenna,
26 Barents Sea) using the marine methanotroph *Methyloprofundus sedimenti*, and analyzed *N.*
27 *labradorica* cytology via Transmission Electron microscopy (TEM). We hypothesized that *M.*
28 *sedimenti* would be visible post experiment in degradation vacuoles, as evidenced by their
29 ultrastructure. Sediment grains (mostly clay) occurred inside one or several degradation vacuoles
30 in all foraminifers. In 24% of the specimens from the feeding experiment degradation vacuoles
31 also contained bacteria, although none could be confirmed to be the offered *M. sedimenti*.
32 Observations of the apertural area after 20-h incubation revealed three putative methanotrophs,
33 close to clay particles, based on bacterial ultrastructural characteristics. Furthermore, we noted the
34 absence of bacterial endobionts in all examined *N. labradorica* but confirmed the presence of
35 kleptoplasts, which were often partially degraded. In sum, we suggest that *M. sedimenti* can be
36 consumed via untargeted grazing in seeps and that *N. labradorica* can be generally classified as a
37 deposit feeder at this Arctic site.

38

39 benthic foraminifera – feeding experiment – grazing - marine methanotrophs – Arctic methane
40 seeps– transmission electron microscopy – ultrastructure – kleptoplasts- protist – molecular
41 identification

42 1. Introduction

43 In methane seep sites, the upward migration of methane affects the pore-water chemistry of near-
44 surface sediments, where benthic foraminifera live (e.g. Dessandier et al., 2019). Extremely light
45 isotopic signals of $\delta^{13}\text{C}$ have been measured in seep-associated foraminiferal calcite tests (Wefer
46 et al., 1994; Rathburn et al., 2003; Hill et al., 2004b; Panieri et al., 2014). Studies specifically
47 looking at living (rose bengal stained) foraminiferal tests support the hypothesis that the carbon
48 isotopic composition is strongly influenced by the porewater DIC (McCorkle et al., 1990a).
49 Interspecific $\delta^{13}\text{C}$ differences between species with similar depth indicate sometimes taxon-
50 specific “vital” effects (McCorkle et al., 1990a). Those “vital” effects describe the biology of the

51 different species, which could reflect different feeding patterns. It has been suggested that
52 *Nonionella auris* is an indicator of methane release and possibly ingests ^{13}C -depleted methane
53 oxidizing bacteria (Wefer et al., 1994). Recently, *Melonis barleeanus* (Williamson, 1858)
54 collected from an active methane seep site was found to be closely associated with putative
55 methanotrophs (Bernhard and Panieri, 2018), providing impetus to examine feeding habits of
56 foraminifera living in or around methane seeps.

57 Methanotrophs produce the biomarker diploterol, which has an extremely light $\delta^{13}\text{C}$ signature
58 (-60 ‰) (Hinrichs et al., 2003). Our hypothesis is that if foraminifera ingest methanotrophs, $\delta^{13}\text{C}$
59 values of foraminiferal cytoplasm should be altered by their diet. Experiments using a high-
60 pressure culturing system revealed the difficulty to measure the sensitive relationship between
61 methane exposure and the foraminifera *Cibicides wuellerstorfi*. However, it was shown in one
62 experiment using entire cores that a methane source was reflected in $\delta^{13}\text{C}$ of foraminiferal calcite
63 (Wollenburg et al., 2015). It is also not yet conclusive if diet can influence foraminiferal calcite,
64 as new calcite did not form during experiments (Mojtahid et al., 2011).

65 Another hypothesis to explain extremely light $\delta^{13}\text{C}$ values recorded in benthic foraminiferal calcite
66 is that foraminifera assimilate carbon as ^{13}C -depleted methane-derived DIC, which would lead to
67 extremely light $\delta^{13}\text{C}$ values. The possibility that ^{13}C -depleted DIC from the pore water can be
68 assimilated by foraminifera is currently debated. Some studies suggest it is not possible (Herguera
69 et al., 2014), while others assert the feasibility that foraminifera calcify close to seeps (Rathburn
70 et al., 2003; Hill et al., 2004a; Panieri et al., 2014). The problem lies in the calcite tests, and the
71 difficulty to assess the time of death of these protists in the sediment. Several studies found that the
72 lightest isotopic $\delta^{13}\text{C}$ values were measured in tests coated by methane-derived authigenic
73 carbonate (MDAC) overgrowth, which happens after the death of the foraminifer (Torres et al.,
74 2010; Panieri et al., 2014; Consolaro et al., 2015; Panieri et al., 2017; Schneider et al., 2017).
75 However, light $\delta^{13}\text{C}$ values remain in many tests after MDACs are removed (Panieri et al., 2014)
76 and have been measured also in primary calcite, without MDACs, from tests in methane-rich
77 environments (e.g. Mackensen, 2008; Dessandier et al., 2019). These observations again point to
78 the role of food influencing the cytoplasmic $\delta^{13}\text{C}$.

79 Foraminifera play an important role in the carbon cycle on the deep seafloor (Nomaki et al., 2005)
80 where feeding behavior and food preference vary with species (Nomaki et al., 2006). Selected
81 species of deep-sea benthic foraminifera have been shown to feed selectively on ^{13}C -labeled algae

82 from sedimentary organic matter, but unselectively on ^{13}C -labeled bacteria of the strain *Vibrio*
83 (Nomaki et al., 2006). A study from the seafloor around Adriatic seeps suggested that $\delta^{13}\text{C}$ of
84 foraminiferal cytoplasm could be influenced by feeding on the sulfur-oxidizing bacterium
85 *Beggiatoa*, whose abundance was also positively correlated with foraminiferal densities (Panieri,
86 2006). Generally, some foraminifera can ingest dissolved organic matter (DOM); some are
87 herbivorous, carnivorous, suspension feeders and most commonly deposit feeders (reviewed in
88 Lipps, 1983). Deposit feeders are omnivorous, gathering fine-grained sediment (e.g., clay) and
89 associated bacteria, organic detritus (dead particulate organic material) and, if present, diatom cells
90 using their pseudopodia. Based on the ultrastructure of the diet found in vacuoles several species
91 of foraminifera from different habitats have already been classified to be deposit feeders (Goldstein
92 and Corliss, 1994).

93 Here we investigate if *Nonionellina labradorica* would feed in a short-term feeding experiment on
94 the marine methanotroph *Metyloprofundus sedimenti* and compare its ultrastructure on
95 experimental specimens and field specimens. *Nonionellina labradorica* is an abundant species in
96 the North Atlantic (Cedhagen, 1991) and occurs together with *N. digitata* in Svalbard fjord
97 sediments (Hald and Korsun, 1997; Shetye et al., 2011; Fossile et al., 2020). In addition to its wide
98 distribution, it is an especially interesting experimental species for feeding studies because it hosts
99 kleptoplasts, *i.e.* sequestered chloroplasts, of diatom origin inside its cytoplasm (Cedhagen, 1991;
100 Jauffrais et al., 2019b). *Nonionellina labradorica*'s aperture shows a specific ornamentation,
101 possibly a morphological adaptation to this “predatory” mode of life for obtaining the kleptoplasts
102 (Bernhard and Bowser, 1999). Denitrification has been speculated for *N. labradorica* (reviewed in
103 Charrieau et al., 2019), because the foraminiferal genus *Nonionella* can denitrify, which was
104 demonstrated on two species (Risgaard-Petersen et al., 2006; Choquel et al., 2021), but not yet on
105 *N. labradorica*. Our study analyzed contents of the degradation vacuoles of this species from an
106 active methane-emitting site in the Arctic (Storfjordrenna, Barents Sea) before and after a feeding
107 experiment.

108 **2. Materials and methods**

109 **2.1. Site description and sampling living foraminifera**

110 The sampling site was located app. 50 km south of Svalbard at 382m water depth at the mouth of
111 Storfjordrenna (Serov et al., 2017). The site is characterized by several large gas hydrate pingos

(GHP), which actively vent methane over an area of 2.5 km². Our samples were taken at GHP3, which is referred to as an underwater gas hydrate-bearing mound (Hong et al., 2017; Hong et al., 2018). GHP3 is a ~500-m diameter, 10-m tall mound that actively vents methane (Fig. 1). Marine sediment samples were collected during CAGE cruise 18-05 supported by the research vessel *Kronprins Haakon* in October 2018 and sampled by the Remotely Operated Vehicle (ROV) *Ægir*. A blade corer BLC18 (surface dimensions 27 x 19 cm, Fig. 1c) was used to retrieve marine sediment in the vicinity of bacterial mats (GPS 76°6'23.7"N 15°58'1.7"E). Once onboard the blade corer was immediately sampled to retrieve living (cytoplasm containing) foraminifera using a small aquarium hose targeting the first cm (~0-1 cm). The sediment was collected in petri dishes and wet sieved to a size range of 250-500 µm. The species *N. labradorica*, which was abundant in that layer, was subsequently used for a feeding experiment described in detail below.

123

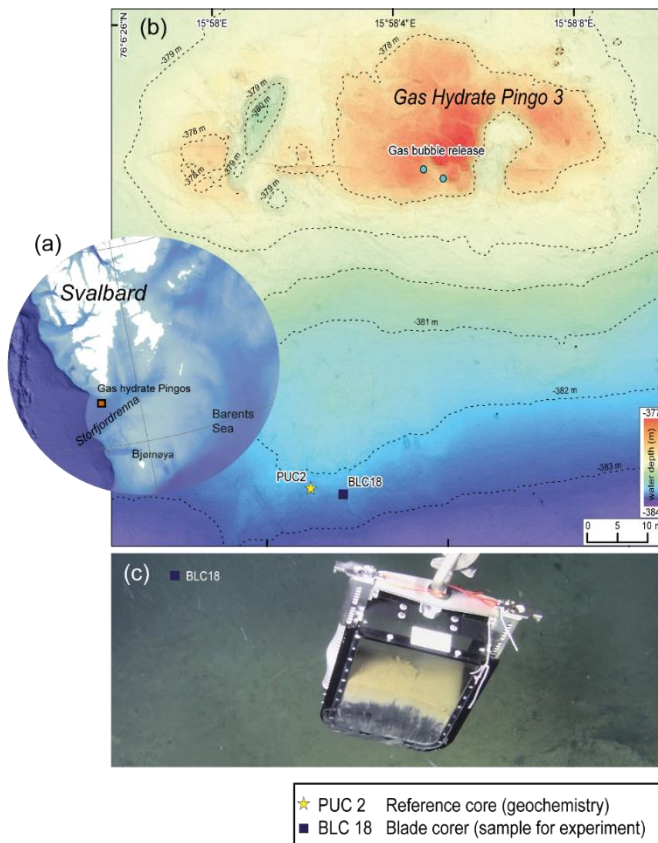


Figure 1. Description of the sampling site Gas Hydrate Pingo 3 (GHP3), a gas-hydrate bearing mound, located in Storfjordrenna Barents Sea. (a) Map illustrating Svalbard Archipelago and the sampling site, app. 50 km offshore. (b) Map of sampling site GHP3, active gas bubble release is marked on the top of the underwater mount, yellow star indicates location of push corer PUC2 (geochemical analyses), black square indicates location of BLC18 (sediment source for experiment). (c) Underwater image of retrieval of BLC18 taken by ROV camera illustrating the coloration of sediment with the sea-floor visible in background.

124 **2.2. Geochemistry of the study site**

125 For geochemical analysis of the study site a push corer (PUC2; henceforth referred to as
126 geochemistry core) was taken to obtain measurements of $\delta^{13}\text{C}_{\text{DIC}}$ and sulfate, because blade corer
127 (BLC18) did not allow those measurements. PUC2 was taken in close vicinity to BLC18, ~5m
128 apart (see Figure S1). Pore-water samples were taken from PUC2 using rhizons that were inserted
129 through pre-drilled holes in the core tube at intervals of 1 cm (Table S1). Acid washed 20-ml
130 syringes were attached to the rhizons for pore water collection. Depending on the amount of pore
131 water collected, the samples were split for $\delta^{13}\text{C}_{\text{DIC}}$ and sulfate measurements. To the samples, 10
132 μL of saturated HgCl_2 (aqueous) was added to stop microbial activity and stored in cold conditions
133 (5°C). A ThermoScientific Gasbench II coupled to a ThermoScientific MAT 253 IRMS at the
134 Stable Isotope Laboratory (SIL) at CAGE, UiT was used to determine $\delta^{13}\text{C}_{\text{DIC}}$ of the pore-water.
135 Anhydrous phosphoric acid was added to small glass vials (volume 4.5 mL), that were closed and
136 flushed with helium 5.0 gas before the pore-water sub-sample was measured. A porewater sub-
137 sample (volume 0.5 mL) was then added through the septa with a syringe needle, followed by
138 equilibration for 24 h at 24°C to liberate the CO_2 gas. Three solid calcite standards with a range of
139 +2 to -49 ‰ were used for normalization to $\delta^{13}\text{C}$ -VPDB. Correction of measured $\delta^{13}\text{C}$ by -0.1 ‰,
140 was done to account for fractionation between (gas) and (aqueous) in sample vials. Instrument
141 precision for $\delta^{13}\text{C}$ on a MAT253 IRMS was +/- 0.1 ‰ (SD). Sulfate was measured with a Metrohm
142 ion chromatography instrument equipped with column Metrosep A sup 4 and eluted with 1.8
143 mmol/L Na_2CO_3 + 1.7 mmol/L NaHCO_3 at the University of Bergen.

144 **2.3. Culturing of the marine methanotroph *M. sedimenti***

145 *Methyloprofundus sedimenti* PKF-14 had been previously isolated from a water-column sample
146 collected at Prins Karls Forland, Svalbard in the laboratory at UiT in Tromsø. *Methyloprofundus*
147 *sedimenti* were cultured in 10-ml batches of a 35:65 mix of 1/10 Nitrate Mineral Salt medium
148 (NMS) and sterile filtered sea water using 125-mL Wheaton® serum bottles with butyl septa and
149 aluminum crimp caps (Teknolab®). Methane was injected to give a headspace of 20% methane in
150 air, and the bottles were incubated without shaking at 15°C in darkness. Purity of the cultures and
151 cell integrity was verified by microscopy and by absence of growth on agar plates with a general
152 medium for heterotrophic bacteria (tryptone, yeast extract, glucose and agar).

153 **2.4. Experimental setup**

154 On the ship, *Nonionellina labradorica* (Fig. 2a,b) specimens showing dark greenish brown
155 cytoplasm were picked using sable artist brushes under a stereomicroscope immediately after wet
156 sieving the sediment using natural seawater delivered from the ship pump. Living specimens had
157 a partly inorganic covering surrounding the test, which was gently removed using fine artist
158 brushes. Those so-called cysts are nothing unusual with many foraminiferan taxa (Heinz et al.,
159 2005).

160 Our specimens were subsequently rinsed twice in filtered artificial seawater to remove any
161 sediment before placing them into the experimental petri dishes. Care was taken that those were
162 minimally exposed to light during preparation of the experiment, as kleptoplasts are known to be
163 highly light sensitive in this foraminifer (Jauffrais et al., 2019b).

164 The experiment with *M. sedimenti* was conducted for a total duration of 20-h to resemble previous
165 experiments on *N. labradorica* using transmission electron microscopy and nanometre-scale
166 secondary ion mass spectrometry isotopic imaging (TEM-NanoSIMS) (Jauffrais et al., 2019b),
167 and included two more time points at 4 and 8 h. A short pre-experimental phase (2-4 h) was
168 included before the start of the feeding experiment, to allow specimens to acclimate. During the
169 pre-experimental phase specimens were not fed and resided in the petri dishes to adjust to the
170 experimental conditions. The feeding experiment consisted of several small petri dishes (3.5 cm
171 Ø, 3 mL) each containing five *N. labradorica* in ASW at ambient salinity 35 (Red Sea Salt). Petri
172 dishes were sealed with Parafilm® and covered with aluminum foil and placed inside the incubator
173 in complete darkness. Temperature inside the chamber was maintained at 2-3°C, which is within
174 the range of the site's bottom-water temperature (-1.8 – 4.6°C) (Hong et al., 2017). The feeding of
175 *M. sedimenti* was performed once at the beginning of the experiment by adding 100 µL of culture
176 to 3 mL of artificial seawater to produce a final concentration of ~1E10⁶ bacteria / mL in each petri
177 dish. Previously conducted feeding studies were used as guides: Muller and Lee (1969) used 1E10⁴
178 bacteria/mL seawater and Mojtabahid et al. (2011) used 4E10⁸ bacteria/mL seawater.

179 Five foraminifera, which served as initial/field specimens (Table 1), were fixed without *M.*
180 *sedimenti* incubation. The respective petri dishes were incubated for 4, 8 and 20 h to determine if
181 incubation duration influenced response of the foraminifera to the methanotroph. One petri dish
182 containing five foraminifera, which were un-fed and fixed at 20 h, served as a negative “control”.
183 After the end of the respective incubation times, each foraminifer was picked with a sterilized fine
184 artist brush, which was cleaned in 70% ethanol between each specimen, and placed individually
185 into a fixative solution (4% glutaraldehyde and 2% paraformaldehyde dissolved in ASW).

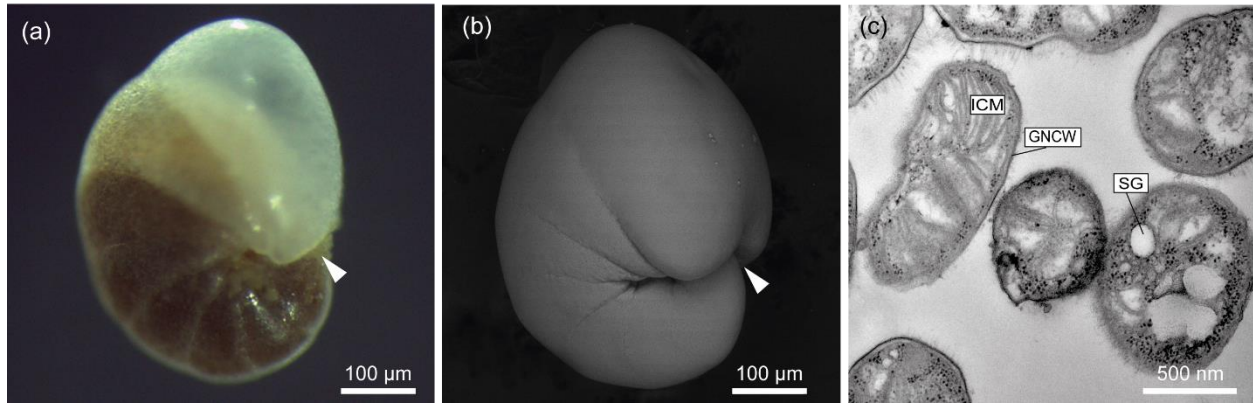


Figure 2 Exemplary illustration of *Nonionellina labradorica*, utilized in this study. (a) Reflected light microscopy image from a specimen directly after sampling, white arrowhead indicates aperture location. (b) Scanning electron image from a specimen before molecular analysis was performed, white arrowhead indicates aperture location. (c) Transmission electron microscopy image of a culture of *Methyloprofundus sedimenti*, the marine methanotroph used in the feeding experiment. The characteristic features for methanotroph identification is the typical type I intracytoplasmic membranes (ICM). Furthermore, other internal structures visible are storage granules (SG), and a gram-negative cell wall (GNCW).

186 2.5. Transmission Electron microscopy (TEM) preparation

187 Samples of *N. labradorica* preserved in fixative solution were transported to the University of
188 Angers, where they were prepared for ultrastructural analysis using established protocols
189 (Lekieffre et al., 2018). Four embedded foraminiferal cells per treatment were sectioned using an
190 ultramicrotome (Leica® Ultracut S) equipped with a diamond knife (Diatome®, ultra 45°). Grids
191 were stained using UranyLess® EM Stain (EMS, USA). Ultra-thin sections (70 nm) were observed
192 with a JEOL JEM-1400 TEM at the SCIAM facility, University of Angers.
193 To document the ultrastructure of *Methyloprofundus sedimenti*, a sub-sample of the culture used
194 for experiments was imaged with TEM (Fig. 2c). To do so, an exponentially growing culture was
195 collected, centrifuged, pre-fixed with 2.5 % (w/v) glutaraldehyde in growth medium overnight,

196 washed in PBS (Phosphate Buffered Saline), then post fixed with 1% (w/v) aqueous osmium
197 tetroxide for 1.5 hours at room temperature. After dehydration in an ethanol series, the samples
198 were embedded in an Epon equivalent (Serva) epoxy resin. Ultra-thin sections were cut on a Leica
199 EM UC6 ultramicrotome, and stained with 3 % (w/v) aqueous uranyl acetate followed by staining
200 with lead citrate (Reynolds, 1963) at 20 °C for 4–5 min. The samples were examined with a JEOL
201 JEM-1010 transmission electron microscope at an accelerating voltage of 80 kV with a Morada
202 camera system at the Advanced Microscopy Core Facility (AMCF), Faculty of Health Science,
203 UiT The Arctic University of Norway.

204 **2.6. Foraminifera ultrastructural observation and image processing**

205 Four specimens per experimental time point (initials, 4, 8 and 20 h) plus one un-fed (control)
206 specimen were examined with the TEM. From each specimen, a minimum of 50 TEM images was
207 taken, including images detailing the degradation vacuoles (app. 5-27 images per specimen).
208 Before the ultrastructure was examined in detail, an overview images was created of each section
209 to illustrate number of chambers and size of the specimen. Images were blended together using
210 Photoshop CS5 (see Fig. 4-5a). Thereafter, the ultrastructure was examined at different parts of
211 the cell: (a) in the interior to document vitality, (b) on degradation vacuoles to determine their
212 contents, and (c) at the exterior to survey for microbes entrained in remnant “reticulopodial trunk”
213 material. All images made during the observations of the TEM sections are deposited at Zenodo
214 (doi: 10.5281/zenodo.6941739).

215 **2.7. Molecular genetics and morphology**

216 DNA metabarcoding and morphological documentation were performed on 13 specimens of *N.*
217 *labradorica*. Briefly, live specimens were dried on micropaleontological slides and transported in
218 a small container, cooled with ice-pads to the University of Angers. All specimens were imaged
219 for morphological analysis using a Scanning Electron Microscope (SEM; EVOLS10, ZEISS, Fig.
220 S1) followed by individually extracting total DNA in DOC buffer (Pawlowski, 2000). To amplify
221 foraminiferal DNA, a hot start PCR (2 min. at 95°C) was performed in a volume of 25µl with 40
222 cycles of 30 s at 95°C, 30 s at 50°C and 2 min at 72°C, followed by 10 min at 72°C for final
223 extension. Primers s14F3 and sB were used for the first PCR and 30 cycles at an annealing
224 temperature of 52°C (other parameters unchanged) for the nested PCR with primers s14F1 and J2
225 (Pawlowski, 2000; Darling et al., 2016). Positive amplifications were sequenced directly with the

226 Sanger method at Eurofins Genomics (Cologne, Germany). For taxonomic identification, DNA
227 sequences were compared first with BLAST (Basic Local Alignment Search Tool) (Altschul et al.,
228 1997) and then within an alignment comprising other Nonionids implemented in SeaView (Gouy
229 et al., 2010) and corrected manually.

230 **3. Results**

231 **3.1. Sample description and geochemistry of the study site**

232 The visual observation of the sediments within the blade corer BLC18 immediately after sampling
233 (Fig. 1c) indicated that the sediment appeared light grey – yellowish in the upper part until app. 13
234 cm and dark brown from app. 13 cm to the bottom. The sulfate measured in the pore water of the
235 geochemistry core (PUC2) declined from ~2750 ppm at the sediment-water interface to ~706 ppm
236 at approximately 13 cm (see Fig. S1, Table S1). A decline in sulfate concentration indicates that
237 the anaerobic oxidation of methane (AOM) occurred at app. 13 cm depth. The SMTZ (Sulfate
238 Methane Transition Zone) characterized by a DIC value of -32‰ at app. 13 cm sediment depth
239 can be considered shallow on the global average (Egger et al., 2018).

240 **3.2. Ultrastructure of methanotroph culture used in the feeding experiment**

241 Transmission Electron Microscopy was performed on culture aliquots to allow morphological
242 comparison to previously published work (Tavormina et al., 2015). *Methyloprofundus sedimenti*
243 strain PKF-14 cells are coccoid to slightly elongated shape and is characterized by typical type I
244 stacked intracytoplasmic membranes (ICM) (Fig. 2c). It has storage granules (SG) and a gram-
245 negative cell wall (GNCW), which are not uniquely charactersitic of methanotrophs (Fig. 2c).
246 Additionally, 16S rRNA gene sequencing was performed (data not shown) to confirm it to be
247 similar to the published *Methyloprofundus sedimenti* (Tavormina et al., 2015).

248 **3.3. Foraminiferal ultrastructure from an Arctic seep environment**

249 **3.3.1 General ultrastructure**

250 All 17 specimen examined for ultrastructure were considered living at the time of observation (Fig.
251 3), as the mitochondria had characteristic double membranes and occasionally visible cristae
252 (Nomaki et al., 2016). Cytoplasm exhibited several vacuoles and kleptoplasts concentrated in the
253 youngest chambers (Fig. 3a) and, in some specimens, a nucleus with nucleoli was visible (Fig. 3b).
254 Kleptoplasts were numerous throughout the cytoplasm and occurred in the form of a single

255 chloroplast (Fig. 3a-b), or as double chloroplasts (Fig. S2a-d). Not all kleptoplasts were intact;
256 some showed peripheral degradation of the membranes indicated by an increasing number of white
257 areas between pyrenoid, lamella and thylakoids (Fig. S2a-d). The mitochondria occurred often in
258 small clusters of two to five throughout the cytoplasm and were oval, round or kidney-shaped in
259 cross section (Fig. 3e-f). Peroxisomes in *N. labradorica* occurred mostly as pairs (Fig. 3c) or small
260 clusters of 3-4 spherical organelles (Fig. S3a). Sometimes, but not always, peroxisomes were
261 associated with endoplasmic reticulum (Fig. S3b) but could also occur alone. Golgi apparatus (Fig
262 3d) had intact membranes, often occurring near mitochondria.

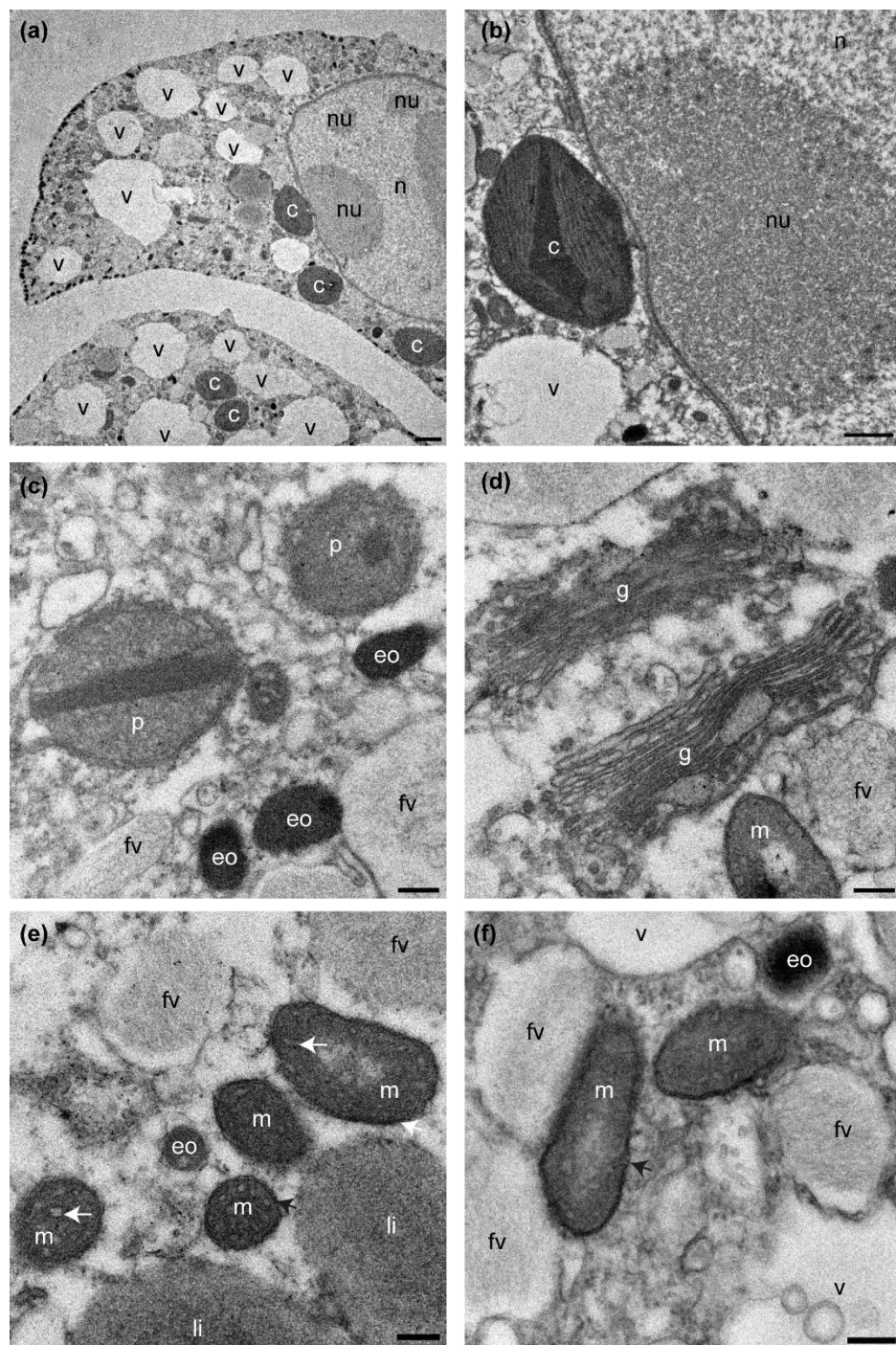


Figure 3 Transmission electron micrographs showing cellular ultrastructure of *N. labradorica*. (a) Cytoplasm showing parts of two chambers, with nucleus with nucleoli, vacuoles and several kleptoplasts, (b) nuclear envelope, nucleoli, and kleptoplasts, (c) peroxisomes and electron opaque bodies, (d) Golgi, (e-f) mitochondria. V=vacuole, c=kleptoplast, nu=nucleoli, n=nucleus p=peroxisome, eo=electron opaque body, m=mitochondrion, fv=fibrillar vesicle, li=lipid droplet. Scales: (a) 2 μ m, (b) 1 μ m, (c-f) 200 nm

264 **3.3.2 Ultrastructure of aperture-associated bacteria**

265 In total, three putative methanotrophs were identified in the vicinity of two specimens (sample
 266 E39, Fig. 4; E37, Fig. 5). These microbes were identified adjacent to reticulopodial remains (Fig.
 267 4b). As an aid for identification of *M. sedimenti* we used the characteristics shown in the literature
 268 (Tavormina et al., 2015) and our own TEM observation obtained from *M. sedimenti* culture (Fig.
 269 2c). As noted, *Methyloprofundus sedimenti* is characterized by a typical type I intracytoplasmic
 270 stacked membrane (ISM). Other characteristics, which are not specific for methanotrophs included
 271 storage granules (SG) and a typical gram-negative cell wall (GNCW) (Fig. 2c). On specimen E39
 272 from the 20 h treatment, we found the methanotroph exhibiting the clearest internal structure,
 273 having both typical type I intracytoplasmic stacked membranes (ISM) and SG (Fig. 4c).
 274

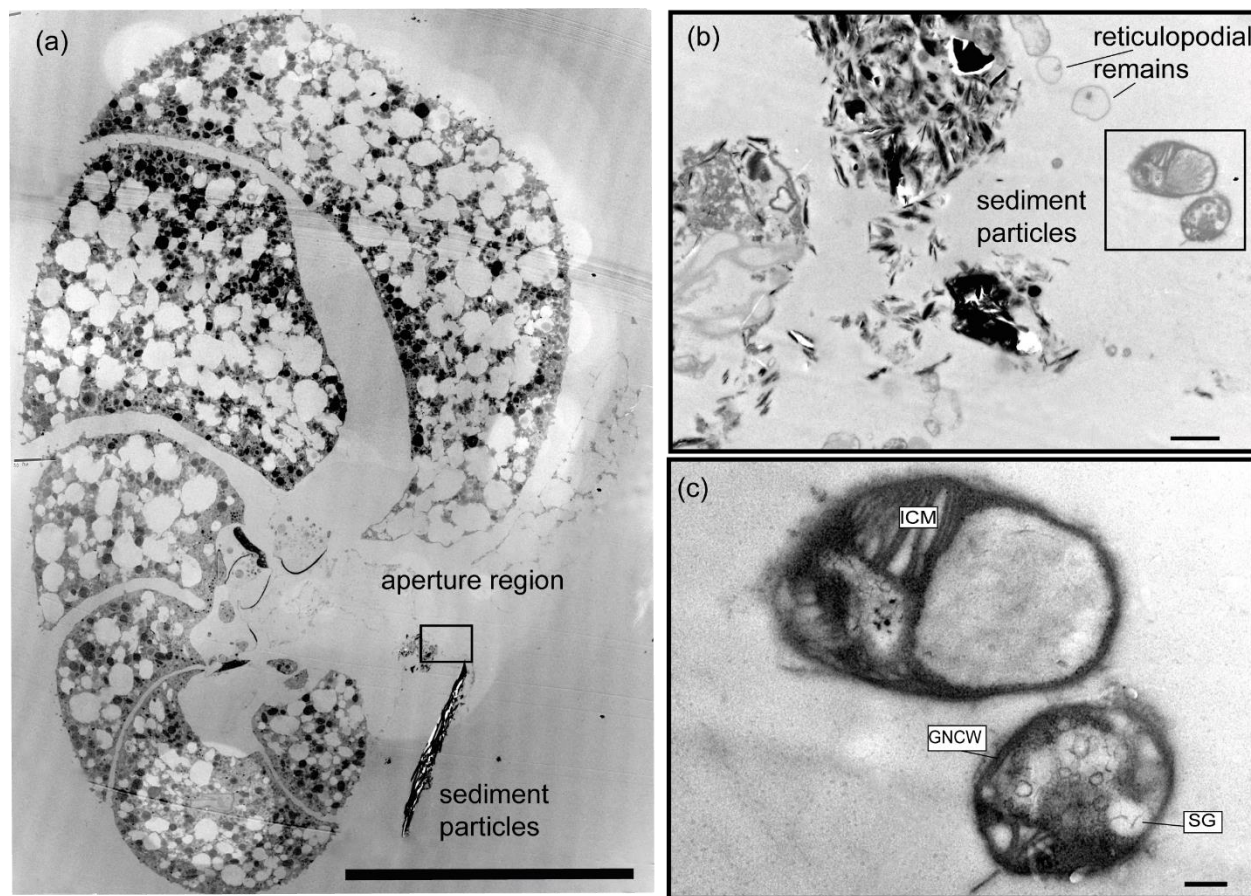
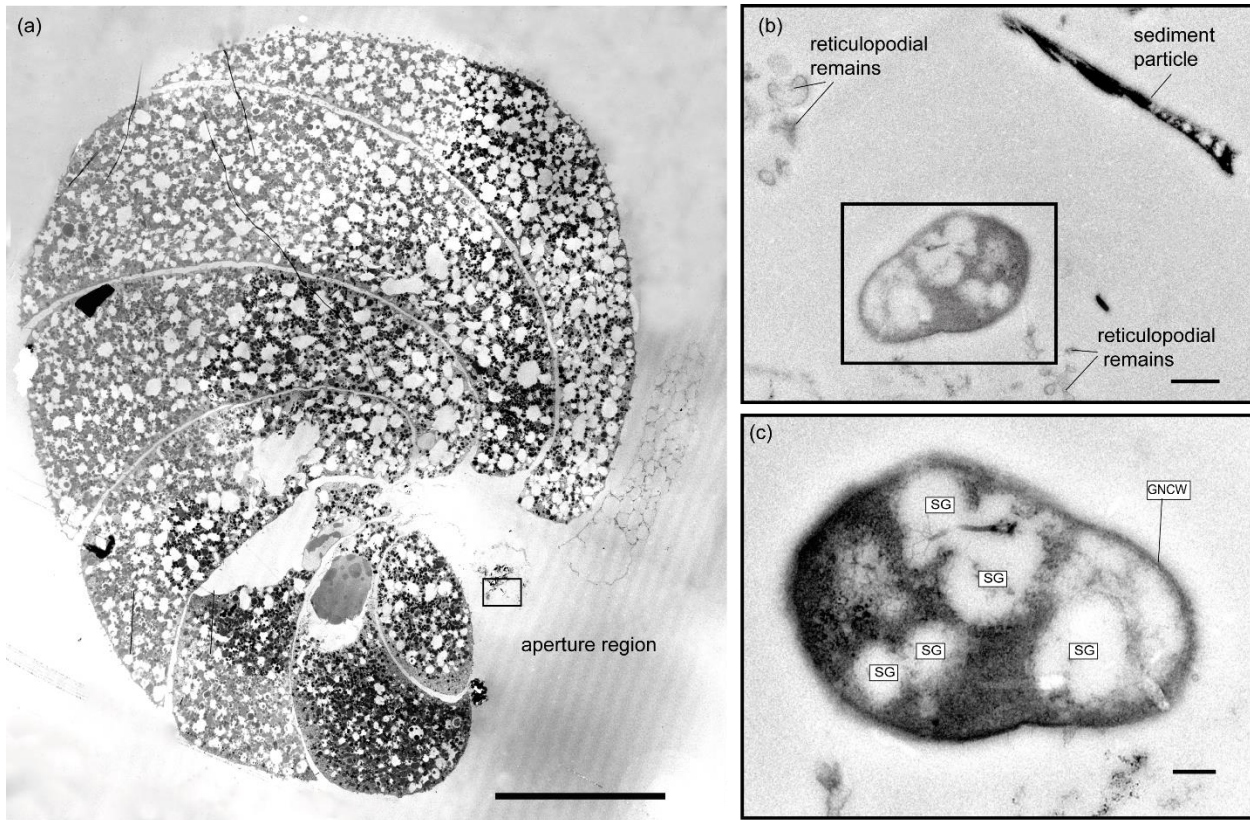


Figure 4 Transmission electron micrographs of *N. labradorica* from 20 h treatment (sample E39) (a) Stitched cross section of TEM images showing location of methanotroph at the aperture region (black rectangle is the location of image shown in panel b) (b) Location of two putative methanotrophs next to sediment particles and putative reticulopodial remains (black rectangle is location of image shown in panel c) (c) Close up of two putative methanotrophs revealing detailed feature for identification, such as typical type I stacked intracytoplasmic membranes (ICM), and other characteristics, such as storage granules (SG), and gram-negative cell wall (GNCW), scale bars: a: 100 μ m, b: 1 μ m, c: 200 nm.



275

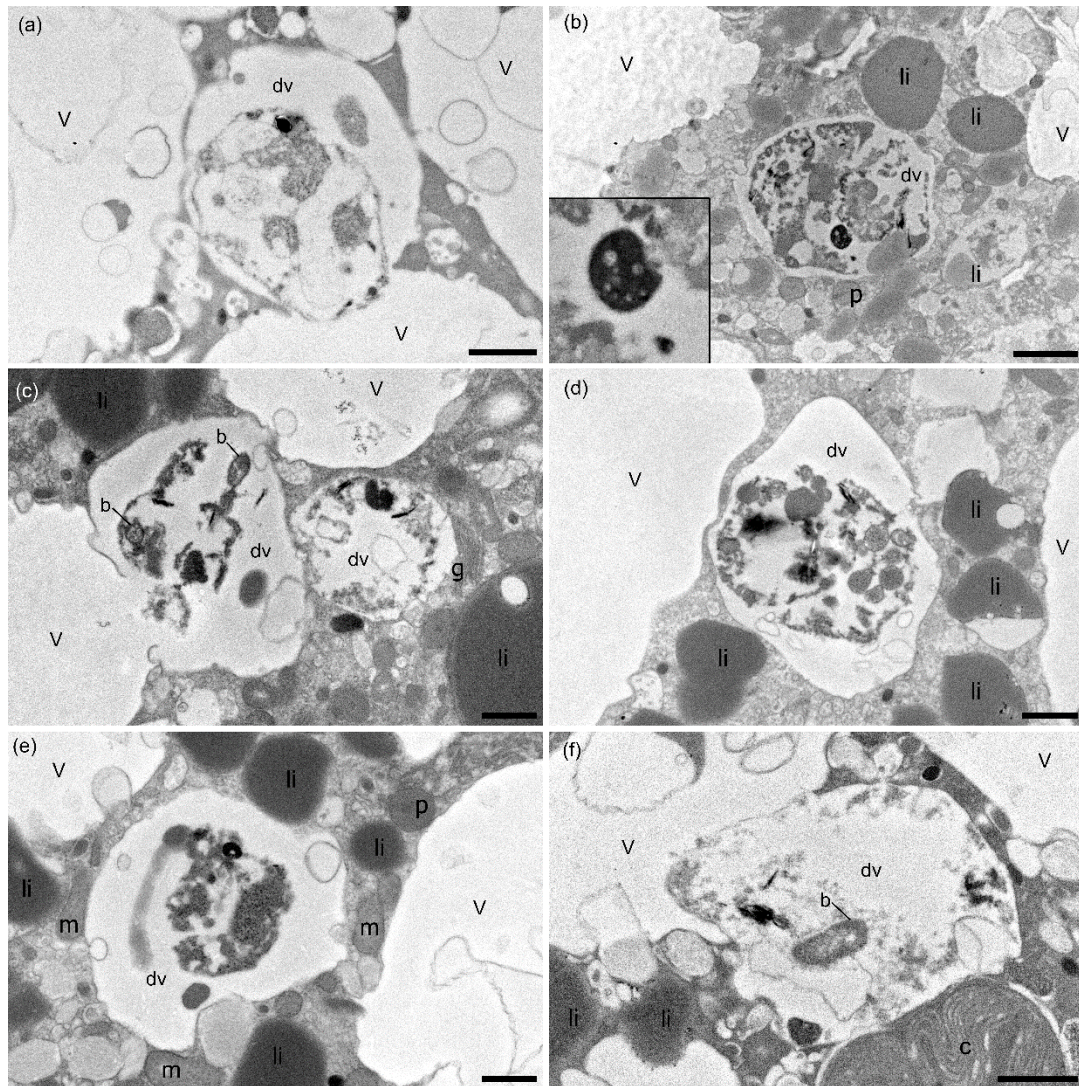
Figure 5 Transmission electron micrographs of *N. labradorica* from 20 h treatment (sample E37) (a) Stitched cross section of TEM images showing location of putative methanotroph (black rectangle) at the aperture region. (b) Location of the putative methanotroph next to sediment particles and sections of the putative reticulopodial remains (c) Close up of putative methanotroph showing several SG throughout its cell, scale bars: a: 100 μ m, b: 0.5 μ m, c: 200 nm.

276

277 3.3.3 Contents of degradation vacuoles

278 Digestive vacuoles and food vacuoles are often summarized as degradation vacuoles in the
 279 literature (Lekieffre et al., 2018) and this makes sense for our study as well. A degradation vacuole
 280 is a vacuole where enzymatic activities degrade contents, often making them unidentifiable (Bé et
 281 al., 1982; Hemleben et al., 2012). Sediment particles were present in many degradation vacuoles.
 282 The sediment grains were easy to recognize in the TEM image as angular grains inside the
 283 vacuoles, next to organic debris, which can have many different shapes. Each specimen had at
 284 least one degradation vacuole and mostly several, which were filled with sediment particles (Table
 285 1). If a sediment particle was visible, the vacuole was defined as a degradation vacuole (dv), and
 286 if it was not and empty then it was defined as a standard vacuole (v) (Fig. 6). The observed
 287 entrained sediment particles were platelets, likely clay from the seafloor, and hence show that the
 288 vacuole must contain foreign objects, around which degradation processes have started. Four of

289 17 specimens examined (23%) had one or more bacteria of various sizes inside their degradation
290 vacuoles next to sediment particles (Fig 6 c, f).



291

Figure 6 TEM micrographs of *N. labradorica* showing degradation vacuoles containing miscellaneous items, including bacteria (b), inorganics (clay platelets) and unidentifiable remains after 4h incubation, which are shown enlarged in the left side of the image in a zoom window (a,b; specimens E27, E28, respectively); after 8h incubation (c,d; specimen E14), after 20h incubation (e,f; specimens E36, E37, respectively). v=vacuole, dv=degradation vacuole, c=kleptoplast, p=peroxisome, m=mitochondrion, li=lipid, g= Golgi. Scales: (a, c-f) 1 μ m, (b) 2 μ m.

292 3.4. Foraminiferal genetics

293 Six of 13 specimens analyzed for genetics were positively amplified and sequenced (Fig. S4). The
294 sequences are deposited in GenBank under the accession numbers MN514777 to MN514782.
295 When comparing them via BLAST, they were between 98.6% and 99.6% identical to published
296 sequences belonging to foraminifera identified as the morphospecies *N. labradorica*, from the

297 Skagerrak, Svalbard and the White Sea (Holzmann and Pawlowski, 2017; Jauffrais et al., 2019b).
298 Sequences were also included in an alignment comprising other nonionids implemented in
299 Seaview (not shown) and corrected manually to check the BLAST search. This step confirmed the
300 BLAST identification.

301 **4. Discussion**

302 **4.1. Sampling site and geochemistry**

303 The sampling site of blade corer BLC18 was in close proximity (~50 m) to an active methane-vent
304 releasing methane bubbles at the gas hydrate pingo (GHP3) (Serov et al., 2017). At such sites with
305 high methane fluxes, the SMTZ (sulfate methane transition zone) is shallow, as sulfate in the
306 sediment is readily consumed in the first tens of centimeters (Barnes and Goldberg, 1976; Iversen
307 and Jørgensen, 1993) by sulfate-reducing bacteria (SRB) (reviewed in Carrier et al., 2020).
308 Geochemical analysis of PUC2 revealed an SMTZ at app. 13 cm, which is rather shallow (Egger
309 et al., 2018), as it can also be several meters deep in other sites (reviewed in Panieri et al., 2017).
310 Similar geochemical characteristics can be considered at the sampling location of living specimens
311 (BLC18) given the close proximity of the two locations. The geochemical data at PUC2 allows
312 us conclude that the site, where living foraminifera were collected, can be classified as an active
313 methane emission site.

314 **4.2. Possible association with putative methanotrophs**

315 The possible association of *N. labradorica* with methanotrophs was documented via presence of
316 two putative methanotrophs, based on microbial ultrastructure (Tavormina et al., 2015). The
317 documentation of this possible association with putative methanotrophs likely is due to the feeding
318 experiment. However, there is a small possibility that the associated methanotrophs were field-
319 remains. Another benthic foraminifer, *Melonis barleeanus*, has been noted to have clumps of
320 putative methanotrophs at the apertural opening of field-collected specimens (Bernhard and
321 Panieri, 2018). However, the non-selective deposit-feeding behavior of *N. labradorica*, which we
322 describe for this species for the first time, shows that methanotrophs may be ingested via
323 untargeted grazing.

324 **4.3. Degradation vacuoles show large number of sediment particles and few bacteria**

325 Our results of the feeding experiment show that 23% of the examined *N. labradorica* specimens
326 contained bacteria inside their degradation vacuoles. That is not a large proportion compared to
327 presence of sediment particles, which occurred in 100% of the examined foraminifers. From this
328 result, however, we infer that *N. labradorica* at this site is a deposit feeder, feeding on organic
329 detritus and associated bacteria. The bacteria observed in the degradation vacuoles resembled those
330 from other deep-sea foraminifera (*Globobulimina pacifica* and *Uvigerina peregrina*) and the
331 shallow-dwelling genus *Ammonia* (Goldstein and Corliss, 1994). Salt-marsh foraminifera also
332 feed on bacteria and detritus, as observed in TEM studies (Frail-Gauthier et al., 2019). Scavenging
333 on bacteria has also been observed by other foraminifera from intertidal environments such as
334 *Ammonia tepida* or *Haynesina germanica* (Pascal et al., 2008) and is a logical consequence from
335 detritus feeding. Certain foraminifera have been shown to selectively ingest algae/bacteria
336 according to strain (Lee et al., 1966; Lee and Muller, 1973). From laboratory cultures we know
337 that several foraminifera cultures require bacteria to reproduce, as antibiotics inhibited
338 reproduction (Muller and Lee, 1969). Future studies will need to employ additional molecular tools
339 to determine the food contents inside the cytoplasm (e.g. Salonen et al., 2019). For example, a
340 recent study used metabarcoding to assess the contribution of eukaryotic OTUs associated with
341 intertidal foraminifera, revealing that *Ammonia* sp. T6 preys on metazoans, whereas *Elphidium* sp.
342 S5 and *Haynesina* sp. S16 were more likely to ingest diatoms (Chronopoulou et al., 2019).

343 **4.4. General ultrastructure of *N. labradorica* collected in a seep environment**

344 Our observations also included the intact nature of all major organelle types of this species, as this
345 was essential to conclude vitality after the experiment (Nomaki et al., 2016). Mitochondria and
346 kleptoplasts were generally homogeneously distributed throughout the cytoplasm confirming
347 previous observations of six *N. labradorica* from the Gullmar Fjord (Lekieffre et al., 2018;
348 Jauffrais et al., 2019b). If mitochondria are concentrated predominately under pore plugs, it can
349 be an indicator that the electron acceptor oxygen is scarce in their environment, as the pores are
350 the direct connection from the cell to the environment. This has been observed in several other
351 studies where mitochondria were accumulated under pores in *N. stella* (Leutenegger and Hansen,
352 1979) and *Bolivina pacifica* (Bernhard et al., 2010).

353 Even though our study did not focus on kleptoplasts, we could observe that kleptoplasts were
354 occasionally degraded, which could have happened; a) during sampling, b) due to exposure to
355 microscope lights or c) due to the age and condition of kleptoplasts inside the host. Kleptoplasts

356 in *N. labradorica* have been studied in detail describing their diatom origin (Cedhagen, 1991),
357 sensitivity to light and missing photosynthetic functionality (Jauffrais et al., 2019b).

358 **5. Conclusions**

359 Based on the content of degradation vacuoles, we conclude that *N. labradorica* from our study
360 site, an active methane emitting site in the Barents Sea, is a deposit-feeder. It ingests large
361 amounts of sediment particles together with bacteria. On two specimens of the feeding experiment,
362 putative methanotrophs were observed near the *N. labradorica* aperture, suggesting ingestion of
363 *M. sedimenti* via “untargeted grazing”. Further studies are needed on feeding strategies of other
364 paleo-oceanographically relevant foraminifera to detangle the relationship between $\delta^{13}\text{C}$ of
365 foraminiferal calcite, their cytoplasm and dietary composition.

366 **6. Data availability**

367 Datasets containing TEM images are downloadable at Zenodo (doi: 10.5281/zenodo.6941739).
368 Molecular sequence data is deposited at Genbank under the accession numbers MN514777 to
369 MN514782.

370 **7. Sample availability**

371 Samples are available upon request and TEM thinsections archived at the University of Angers.

372 **8. Acknowledgments**

373 We thank the captains, crew members and scientists onboard R/V *Kronprins Haakon* and ROV
374 *Ægir* Team for their assistance; Anne-Grethe Hestnes for growing the methanotroph culture.
375 Florence Manero, Romain Mallet and Rodolphe Perrot at the SCIAM microscopy facility
376 University of Angers are to thank for their expertise with the TEM and SEM. We thank Sunil
377 Vadakkepuliyambatta for helping to prepare the map presented in Figure 1; Sophie Quinchard
378 (LPG-BIAF) for supporting the molecular analysis. Funding was received through the Research
379 Council of Norway, CAGE (Center for Excellence in Arctic Gas Hydrate Environment and
380 Climate, project number 223259) and NORCRUST (project number 255150) to GP, EG, and CS.
381 CS position was funded through the MOPGA (Make Our Planet Great Again) fellowship by
382 CAMPUS France, the NORCRUST project and the University of Angers. JMB was partially
383 supported by US NSF 1634469, WHOI’s Investment in Science Program, and by the Région Pays
384 de la Loire through the FRESCO Project.

385 **9. Author Contributions**

386 Designed the project and experiment: GP, EG, CS; Collected samples: CS, EG; Performed
387 experiment: CS; Sample preparation: CS, HR; TEM observations and interpretations: CS, JMB,
388 EG, CL; Conducted molecular genetics: MSc; Wrote the paper: CS, GP, JMB; Provided critical
389 review and edits to the manuscript: EG, CL, MSv, MSc, HR; Contributed
390 reagents/materials/analysis tools: MSv, MSc, CL.

391 **10. Competing interests**

392 The authors declare that they have no conflict of interest.

393

394 **Table I.** Summary of TEM observations of *Nonionellina labradorica* comparing field specimens
 395 and experimental specimens. Field specimens (initials) were not fed, nor was a non-fed control
 396 preserved after a 20 h incubation. The only putative methanotrophs were observed and imaged in
 397 specimens from the 20 h incubation. Bacteria of unknown origin were described as rod shaped
 398 cells in the degradation vacuoles.

399

Duration of experiment (h)/field samples	Food provided (yes (x)/no)	Sample ID	Cytoplasm: Degradation vacuole Contents		Aperture region: (putative) Methanotrophs
			bacteria	Clay/in-organics	
4	No	E1	no	x	no
	No	E3	no	x	no
	No	E5	no	x	no
	No	E6	no	x	no
	x	E25	no	x	no
	x	E27	x	x	no
	x	E28	no	x	no
	x	E29	no	x	no
	x	E14	x	x	no
	x	E15	no	x	no
8	x	E16	no	x	no
	x	E17	no	x	no
	x	E36	x	x	1 x
	x	E37	x	x	no
20	x	E38	no	x	no
	x	E39	no	x	2 x
	Control (20)	E44	no	x	no

400

401

402

403 **References:**

404

405 Altschul, S. F., Madden, T. L., Schäffer, A. A., Zhang, J., Zhang, Z., Miller, W., and Lipman, D.
406 J.: Gapped BLAST and PSI-BLAST: a new generation of protein database search programs,
407 Nucleic Acids Res., 25, 3389-3402, <https://doi.org/10.1093/nar/25.17.3389>, 1997.

408 Barnes, R. O. and Goldberg, E. D.: Methane production and consumption in anoxic marine
409 sediments, Geology, 4, 297-300, [https://doi.org/10.1130/0091-7613\(1976\)4<297:MPACIA>2.0.CO;2](https://doi.org/10.1130/0091-7613(1976)4<297:MPACIA>2.0.CO;2), 1976.

410

411 Bé, A. W. H., Spero, H. J., and Anderson, O. R.: Effects of symbiont elimination and reinfection
412 on the life processes of the planktonic foraminifer *Globigerinoides sacculifer*, Marine Biology,
413 70, 73-86, <https://doi.org/10.1007/BF00397298>, 1982.

414 Bernhard, J. M. and Bowser, S. S.: Benthic foraminifera of dysoxic sediments: chloroplast
415 sequestration and functional morphology, Earth-Sci. Rev., 46, 149-165,
416 [https://doi.org/10.1016/s0012-8252\(99\)00017-3](https://doi.org/10.1016/s0012-8252(99)00017-3), 1999.

417 Bernhard, J. M. and Panieri, G.: Keystone Arctic paleoceanographic proxy association with
418 putative methanotrophic bacteria, Sci Rep-Uk, 8, 10610, <https://doi.org/10.1038/s41598-018-28871-3>, 2018.

419

420 Bernhard, J. M., Goldstein, S. T., and Bowser, S. S.: An ectobiont-bearing foraminiferan,
421 *Bolivina pacifica*, that inhabits microxic pore waters: cell-biological and paleoceanographic
422 insights, Environmental Microbiology, 12, 2107-2119, 10.1111/j.1462-2920.2009.02073.x,
423 2010.

424 Carrier, V., Svenning, M. M., Gründger, F., Niemann, H., Dessandier, P.-A., Panieri, G., and
425 Kalenitchenko, D.: The Impact of Methane on Microbial Communities at Marine Arctic Gas
426 Hydrate Bearing Sediment, Frontiers in Microbiology, 11, 10.3389/fmicb.2020.01932, 2020.

427 Cedhagen, T.: Retention of chloroplasts and bathymetric distribution in the sublittoral
428 foraminiferan *Nonionellina labradorica*, Ophelia, 33, 17-30,
429 <https://doi.org/10.1080/00785326.1991.10429739>, 1991.

430 Charrieau, L. M., Ljung, K., Schenk, F., Daewel, U., Kritzberg, E., and Filipsson, H. L.: Rapid
431 environmental responses to climate-induced hydrographic changes in the Baltic Sea entrance,
432 Biogeosciences, 16, 3835-3852, 10.5194/bg-16-3835-2019, 2019.

433 Choquel, C., Geslin, E., Metzger, E., Filipsson, H. L., Risgaard-Petersen, N., Launeau, P.,
434 Giraud, M., Jauffrais, T., Jesus, B., and Mouret, A.: Denitrification by benthic foraminifera and
435 their contribution to N-loss from a fjord environment, Biogeosciences, 18, 327-341, 10.5194/bg-
436 18-327-2021, 2021.

437 Chronopoulou, P.-M., Salonen, I., Bird, C., Reichart, G.-J., and Koho, K. A.: Metabarcoding
438 insights into the trophic behavior and identity of intertidal benthic foraminifera, *Frontiers in*
439 *microbiology*, 10, 1169, <https://doi.org/10.3389/fmicb.2019.01169>, 2019.

440 Consolaro, C., Rasmussen, T., Panieri, G., Mienert, J., Bünz, S., and Sztybor, K.: Carbon isotope
441 ($\delta^{13}\text{C}$) excursions suggest times of major methane release during the last 14 kyr in Fram Strait,
442 the deep-water gateway to the Arctic, *Clim. Past*, 11, 669-685, <https://doi.org/10.5194/cp-11-669-2015>, 2015.

444 Darling, K. F., Schweizer, M., Knudsen, K. L., Evans, K. M., Bird, C., Roberts, A., Filipsson, H.
445 L., Kim, J.-H., Gudmundsson, G., Wade, C. M., Sayer, M. D. J., and Austin, W. E. N.: The
446 genetic diversity, phylogeography and morphology of Elphidiidae (Foraminifera) in the
447 Northeast Atlantic, *Mar. Micropaleontol.*, 129, 1-23,
448 <https://doi.org/10.1016/j.marmicro.2016.09.001>, 2016.

449 Dessandier, P.-A., Borrelli, C., Kalenitchenko, D., and Panieri, G.: Benthic Foraminifera in
450 Arctic Methane Hydrate Bearing Sediments, *Frontiers in Marine Science*, 6,
451 <https://doi.org/10.3389/fmars.2019.00765>, 2019.

452 Egger, M., Riedinger, N., Mogollón, J. M., and Jørgensen, B. B.: Global diffusive fluxes of
453 methane in marine sediments, *Nature Geoscience*, 11, 421-425, 10.1038/s41561-018-0122-8,
454 2018.

455 Fossile, E., Nardelli, M. P., Jouini, A., Lansard, B., Pusceddu, A., Moccia, D., Michel, E., Péron,
456 O., Howa, H., and Mojtabid, M.: Benthic foraminifera as tracers of brine production in
457 Storfjorden “sea ice factory”, *Biogeosciences*, 17, <https://doi.org/10.5194/bg-17-1933-2020>,
458 2020.

459 Frail-Gauthier, J. L., Mudie, P. J., Simpson, A. G. B., and Scott, D. B.: Mesocosm and
460 Microcosm Experiments On the Feeding of Temperate Salt Marsh Foraminifera, *J. Foraminifer.
461 Res.*, 49, 259-274, <https://doi.org/10.2113/gsjfr.49.3.259>, 2019.

462 Goldstein, S. T. and Corliss, B. H.: Deposit feeding in selected deep-sea and shallow-water
463 benthic foraminifera, *Deep Sea Research Part I: Oceanographic Research Papers*, 41, 229-241,
464 [https://doi.org/10.1016/0967-0637\(94\)90001-9](https://doi.org/10.1016/0967-0637(94)90001-9), 1994.

465 Gouy, M., Guindon, S., and Gascuel, O.: SeaView version 4: a multiplatform graphical user
466 interface for sequence alignment and phylogenetic tree building, *Mol. Biol. Evol.*, 27, 221-224,
467 <https://doi.org/10.1093/molbev/msp259>, 2010.

468 Hald, M. and Korsun, S.: Distribution of modern benthic foraminifera from fjords of Svalbard,
469 European Arctic, *The Journal of Foraminiferal Research*, 27, 101-122,
470 <https://doi.org/10.2113/gsjfr.27.2.101>, 1997.

471 Heinz, P., Geslin, E., and Hemleben, C.: Laboratory observations of benthic foraminiferal cysts,
472 Mar. Biol. Res., 1, 149-159, 2005.

473 Hemleben, C., Spindler, M., and Anderson, O. R.: Modern planktonic foraminifera, Springer
474 Science & Business Media2012.

475 Herguera, J. C., Paull, C. K., Perez, E., Ussler Iii, W., and Peltzer, E.: Limits to the sensitivity of
476 living benthic foraminifera to pore water carbon isotope anomalies in methane vent
477 environments, Paleoceanography, 29, 273-289, <https://doi.org/10.1002/2013PA002457>, 2014.

478 Hill, R., Schreiber, U., Gademann, R., Larkum, A. W. D., Kuhl, M., and Ralph, P. J.: Spatial
479 heterogeneity of photosynthesis and the effect of temperature-induced bleaching conditions in
480 three species of corals, Marine Biology, 144, 633-640, <https://doi.org/10.1007/s00227-003-1226-1>, 2004a.

482 Hill, T. M., Kennett, J. P., and Valentine, D. L.: Isotopic evidence for the incorporation of
483 methane-derived carbon into foraminifera from modern methane seeps, Hydrate Ridge,
484 Northeast Pacific, Geochimica et Cosmochimica Acta, 68, 4619-4627,
485 <https://doi.org/10.1016/j.gca.2004.07.012>, 2004b.

486 Hinrichs, K.-U., Hmelo, L. R., and Sylva, S. P.: Molecular fossil record of elevated methane
487 levels in late Pleistocene coastal waters, Science, 299, 1214-1217,
488 <https://doi.org/10.1126/science.1079601>, 2003.

489 Holzmann, M. and Pawlowski, J.: An updated classification of rotaliid foraminifera based on
490 ribosomal DNA phylogeny, Mar. Micropaleontol., 132, 18-34,
491 <https://doi.org/10.1016/j.marmicro.2017.04.002>, 2017.

492 Hong, W.-L., Torres, M. E., Carroll, J., Crémère, A., Panieri, G., Yao, H., and Serov, P.:
493 Seepage from an arctic shallow marine gas hydrate reservoir is insensitive to momentary ocean
494 warming, Nat. Commun., 8, 15745, <https://doi.org/10.1038/ncomms15745>, 2017.

495 Hong, W. L., Torres, M. E., Portnov, A., Waage, M., Haley, B., and Lepland, A.: Variations in
496 gas and water pulses at an Arctic seep: fluid sources and methane transport, Geophys. Res. Lett.,
497 45, 4153-4162, <https://doi.org/10.1029/2018GL077309>, 2018.

498 Iversen, N. and Jørgensen, B. B.: Diffusion coefficients of sulfate and methane in marine
499 sediments: Influence of porosity, Geochimica et Cosmochimica Acta, 57, 571-578,
500 [https://doi.org/10.1016/0016-7037\(93\)90368-7](https://doi.org/10.1016/0016-7037(93)90368-7), 1993.

501 Jauffrais, T., LeKieffre, C., Schweizer, M., Jesus, B., Metzger, E., and Geslin, E.: Response of a
502 kleptoplastidic foraminifer to heterotrophic starvation: photosynthesis and lipid droplet
503 biogenesis, FEMS Microbiol. Ecol., 95, 10.1093/femsec/fiz046, 2019a.

504 Jauffrais, T., LeKieffre, C., Schweizer, M., Geslin, E., Metzger, E., Bernhard, J. M., Jesus, B.,
505 Filipsson, H. L., Maire, O., and Meibom, A.: Kleptoplastidic benthic foraminifera from aphotic
506 habitats: insights into assimilation of inorganic C, N and S studied with sub-cellular resolution,
507 Environmental microbiology, 21, 125-141, <https://doi.org/10.1111/1462-2920.14433>, 2019b.

508 Lee, J. J. and Muller, W. A.: Trophic dynamics and niches of salt marsh foraminifera, Am. Zool.,
509 13, 215-223, 1973.

510 Lee, J. J., McEnery, M., Pierce, S., Freudenthal, H., and Muller, W.: Tracer experiments in
511 feeding littoral foraminifera, The Journal of Protozoology, 13, 659-670, 1966.

512 LeKieffre, C., Bernhard, J. M., Mabilleau, G., Filipsson, H. L., Meibom, A., and Geslin, E.: An
513 overview of cellular ultrastructure in benthic foraminifera: New observations of rotalid species in
514 the context of existing literature, Mar. Micropaleontol., 138, 12-32,
515 <https://doi.org/10.1016/j.marmicro.2017.10.005>, 2018.

516 Leutenegger, S. and Hansen, H. J.: Ultrastructural and radiotracer studies of pore function in
517 foraminifera, Marine Biology, 54, 11-16, 10.1007/BF00387046, 1979.

518 Lipps, J. H.: Biotic Interactions in Benthic Foraminifera, in: Biotic Interactions in Recent and
519 Fossil Benthic Communities, edited by: Tevesz, M. J. S., and McCall, P. L., Springer US,
520 Boston, MA, 331-376, 10.1007/978-1-4757-0740-3_8, 1983.

521 Mackensen, A.: On the use of benthic foraminiferal $\delta^{13}\text{C}$ in palaeoceanography: constraints
522 from primary proxy relationships, Geological Society, London, Special Publications, 303, 121-
523 133, <https://doi.org/10.1144/SP303.9>, 2008.

524 Mojtabid, M., Zubkov, M. V., Hartmann, M., and Gooday, A. J.: Grazing of intertidal benthic
525 foraminifera on bacteria: Assessment using pulse-chase radiotracing, J. Exp. Mar. Biol. Ecol.,
526 399, 25-34, <https://doi.org/10.1016/j.jembe.2011.01.011>, 2011.

527 Muller, W. A. and Lee, J. J.: Apparent Indispensability of Bacteria in Foraminiferan Nutrition,
528 The Journal of Protozoology, 16, 471-478, <https://doi.org/10.1111/j.1550-7408.1969.tb02303.x>,
529 1969.

530 Nomaki, H., Heinz, P., Nakatsuka, T., Shimanaga, M., and Kitazato, H.: Species-specific
531 ingestion of organic carbon by deep-sea benthic foraminifera and meiobenthos: In situ tracer
532 experiments, Limnol. Oceanogr., 50, 134-146, <https://doi.org/10.4319/lo.2005.50.1.0134>, 2005.

533 Nomaki, H., Heinz, P., Nakatsuka, T., Shimanaga, M., Ohkouchi, N., Ogawa, N. O., Kogure, K.,
534 Ikemoto, E., and Kitazato, H.: Different ingestion patterns of C-13-labeled bacteria and algae by
535 deep-sea benthic foraminifera, Marine Ecology-Progress Series, 310, 95-108,
536 <https://doi.org/10.3354/meps310095>, 2006.

537 Nomaki, H., Bernhard, J. M., Ishida, A., Tsuchiya, M., Uematsu, K., Tame, A., Kitahashi, T.,
538 Takahata, N., Sano, Y., and Toyofuku, T.: Intracellular Isotope Localization in Ammonia sp.
539 (Foraminifera) of Oxygen-Depleted Environments: Results of Nitrate and Sulfate Labeling
540 Experiments, *Frontiers in Microbiology*, 7, <https://doi.org/10.3389/fmicb.2016.00163>, 2016.

541 Panieri, G.: Foraminiferal response to an active methane seep environment: A case study from
542 the Adriatic Sea, *Mar. Micropaleontol.*, 61, 116-130,
543 <https://doi.org/10.1016/j.marmicro.2006.05.008>, 2006.

544 Panieri, G., James, R. H., Camerlenghi, A., Westbrook, G. K., Consolato, C., Cacho, I., Cesari,
545 V., and Cervera, C. S.: Record of methane emissions from the West Svalbard continental margin
546 during the last 23.500yrs revealed by $\delta^{13}\text{C}$ of benthic foraminifera, *Global and Planetary
547 Change*, 122, 151-160, <https://doi.org/10.1016/j.gloplacha.2014.08.014>, 2014.

548 Panieri, G., Lepland, A., Whitehouse, M. J., Wirth, R., Raanes, M. P., James, R. H., Graves, C.
549 A., Crémère, A., and Schneider, A.: Diagenetic Mg-calcite overgrowths on foraminiferal tests in
550 the vicinity of methane seeps, *Earth and Planetary Science Letters*, 458, 203-212,
551 <https://doi.org/10.1016/j.epsl.2016.10.024>, 2017.

552 Pascal, P.-Y., Dupuy, C., Richard, P., and Niquil, N.: Bacterivory in the common foraminifer
553 Ammonia tepida: Isotope tracer experiment and the controlling factors, *J. Exp. Mar. Biol. Ecol.*,
554 359, 55-61, <https://doi.org/10.1016/j.jembe.2008.02.018>, 2008.

555 Pawlowski, J.: Introduction to the molecular systematics of foraminifera, *Micropaleontology*, 46,
556 1-12, 2000.

557 Rathburn, A. E., Pérez, M. E., Martin, J. B., Day, S. A., Mahn, C., Gieskes, J., Ziebis, W.,
558 Williams, D., and Bahls, A.: Relationships between the distribution and stable isotopic
559 composition of living benthic foraminifera and cold methane seep biogeochemistry in Monterey
560 Bay, California, *Geochemistry, Geophysics, Geosystems*, 4, 2003.

561 Risgaard-Petersen, N., Langezaal, A. M., Ingvardsen, S., Schmid, M. C., Jetten, M. S. M., Op
562 den Camp, H. J. M., Derksen, J. W. M., Piña-Ochoa, E., Eriksson, S. P., Peter Nielsen, L., Peter
563 Revsbech, N., Cedhagen, T., and van der Zwaan, G. J.: Evidence for complete denitrification in a
564 benthic foraminifer, *Nature*, 443, 93, <https://doi.org/10.1038/nature05070>, 2006.

565 Salonen, I. S., Chronopoulou, P.-M., Bird, C., Reichart, G.-J., and Koho, K. A.: Enrichment of
566 intracellular sulphur cycle-associated bacteria in intertidal benthic foraminifera revealed by 16S
567 and aprA gene analysis, *Sci Rep-Uk*, 9, 1-12, <https://doi.org/10.1038/s41598-019-48166-5>, 2019.

568 Schneider, A., Crémère, A., Panieri, G., Lepland, A., and Knies, J.: Diagenetic alteration of
569 benthic foraminifera from a methane seep site on Vestnesa Ridge (NW Svalbard), *Deep Sea
570 Research Part I: Oceanographic Research Papers*, 123, 22-34,
571 <https://doi.org/10.1016/j.dsr.2017.03.001>, 2017.

572 Serov, P., Vadakkepuliyambatta, S., Mienert, J., Patton, H., Portnov, A., Silyakova, A., Panieri,
573 G., Carroll, M. L., Carroll, J., Andreassen, K., and Hubbard, A.: Postglacial response of Arctic
574 Ocean gas hydrates to climatic amelioration, Proceedings of the National Academy of Sciences,
575 114, 6215-6220, 10.1073/pnas.1619288114, 2017.

576 Shetye, S., Mohan, R., Shukla, S. K., Maruthadu, S., and Ravindra, R.: Variability of
577 Nonionellina labradorica Dawson in Surface Sediments from Kongsfjorden, West Spitsbergen,
578 Acta Geologica Sinica - English Edition, 85, 549-558, <https://doi.org/10.1111/j.1755-6724.2011.00450.x>, 2011.

580 Tavormina, P. L., Hatzenpichler, R., McGlynn, S., Chadwick, G., Dawson, K. S., Connan, S. A.,
581 and Orphan, V. J.: Methyloprofundus sedimenti gen. nov., sp. nov., an obligate methanotroph
582 from ocean sediment belonging to the 'deep sea-1' clade of marine methanotrophs, Int. J. Syst.
583 Evol. Microbiol., 65, 251-259, <https://doi.org/10.1099/ij.s.0.062927-0>, 2015.

584 Torres, M. E., Martin, R. A., Klinkhammer, G. P., and Nesbitt, E. A.: Post depositional alteration
585 of foraminiferal shells in cold seep settings: New insights from flow-through time-resolved
586 analyses of biogenic and inorganic seep carbonates, Earth and Planetary Science Letters, 299,
587 10-22, <https://doi.org/10.1016/j.epsl.2010.07.048>, 2010.

588 Wefer, G., Heinze, P. M., and Berger, W. H.: Clues to ancient methane release, Nature, 369, 282,
589 <https://doi.org/10.1038/369282a0>, 1994.

590 Wollenburg, J. E., Raitzsch, M., and Tiedemann, R.: Novel high-pressure culture experiments on
591 deep-sea benthic foraminifera—Evidence for methane seepage-related $\delta^{13}\text{C}$ of Cibicides
592 wuellerstorfi, Mar. Micropaleontol., 117, 47-64, 2015.

593